The correlation of tissue motion within the lung: implications on fiducial based treatments

Ryan L. Smith, Deshan Yang, Andrew Lee, Martin L. Mayse, Dan A. Low, and Parag J. Parikh[a)]
Washington University Medical School, 4921 Parkview Place Campus, Box 8224, St. Louis, Missouri 63110

(Received 9 February 2011; revised 24 August 2011; accepted for publication 3 September 2011; published 19 October 2011)

In radiation therapy many motion management and alignment techniques rely on the accuracy of an internal fiducial acting as a surrogate for target motion within the lung. Although fiducials are routinely used as surrogates for tumor motion, the extent to which varying spatial locations in the lung move similarly to other locations has yet to be quantitatively analyzed. In an attempt to analyze the motion correlation throughout the lung, ten primary lung cancer patients underwent IRB-approved 4DCT scans in the supine position. Deformable registration produced motion vectors for each voxel between exhalation and inhalation. Modeling was performed for each vector and all surrounding vectors within the lung in order to determine the mean 3D Euclidean distance necessary for an implanted fiducial to correlate with surrounding tissue motion to within 3 mm (left lower: 1.7 cm, left upper: 2.1 cm, right lower 1.6 cm, and right upper 2.9 cm). No general implantation rule of where to position a fiducial with respect to the tumor was found as the motion is highly patient and lobe specific. Correlation maps are presented showcasing spatial anisotropy of the motion of tissue surrounding the tumor. © *2011 American Association of Physicists in Medicine*. [DOI: 10.1118/1.3643028]

Key words: lung, motion management, radiation therapy, fiducial marker

I. INTRODUCTION

Radiation therapy often relies on fractionated treatment, which requires repeated patient positioning. Motion associated with respiration can be on the order of centimeters. For targets in the lung and abdomen, respiratory motion complicates accurate radiation delivery.

Cone beam CT imaging provides the spatial location of the tumor, but this technique suffers from poor temporal resolution for real-time guidance applications. In order to mitigate the effects of motion, external surrogates have been employed to monitor the breathing cycle and gate the beam such that it only irradiates during exhalation. While these surrogates offer a noninvasive option for motion management, the degree to which external respiratory surrogates reflect internal tumor motion varies.[1–3]

Recent work has shown that implanted fiducial tumor surrogates are safe and stable throughout the course of treatment. In a study from Kupelian *et al.*, CT imaging was used to assess the proximity between an implanted metal fiducial and the GTV centroid throughout the course of treatment.[4] The average 3D variation in the GTV center relative to the marker was 2.6 mm, with all cases <5 mm. Although tumor shrinkage was apparent as a result of radiation, fiducials in or near tumors were relatively stable throughout treatment. Additionally, there was no incidence of pneumothorax in the six patients that underwent transbronchial implantation.

Real-time applications using internal fiducials as analogues for tumor motion have been developed, and the use of implanted fiducials in or near a target of interest has seen widespread adoption for daily patient alignment.[5–7] We have previously published use of wireless electromagnetic transponders (Calypso Medical®, Seattle WA) for radiation therapy to increase dosimetric accuracy in the presence of respiratory motion.[8–10] The transponder positions are continuously monitored using electromagnetics, and their position with respect to isocenter is known in real-time. In an initial study, the real-time internal fiducial position was used to gate the beam.[8] In later studies, the beam aperture was effectively "moved" using dynamic multileaf collimator (DMLC) tracking in order to follow the real-time position of a transponder.[9,10] The Cyberknife Synchrony system and the ExacTrac x-Ray 6D IGRT system (BRAINLAB) rely on stereoscopic x-ray imaging in order to determine the position of an internal fiducial in real-time.[11,12] A correlation model developed at the start of treatment relates the internal fiducial motion with respect to infrared markers attached to the patient's surface. Intermittent imaging is employed to confirm and continually update the correlation model. Using this position, the beam is moved using a robotic arm and/or gated on/off in order to mitigate the effects of respiratory motion.

The degree to which the motion of an implanted lung fiducial correlates with the motion of a tumor typically deteriorates with increased implantation distance between the fiducial and the tumor. It has been shown that increasing the proximity between an external respiratory sensor and internal target increases the correlation.[13] Similarly, increasing the distance between an implanted fiducial and the target has the potential to increase the error resulting from deformation between the fiducial/target. For fiducials in the lung, bronchoscopic implantation is typically favored over percutaneous implantation due to the reduced risk of pneumothorax.[4] As a result, the proximity of the internal transponder and the target of interest is limited by the bronchial tree structure.

Distal airways are smaller in diameter and limit access to peripheral lesions, which typically exhibit large amplitudes of motion (~1–4 cm).

While the previous studies have investigated the overall fixation of an internal fiducial for lung tumor tracking, there has not been a quantitative assessment of how close a fiducial must be placed with respect to a tumor in order to ensure accurate motion representation. Groundwork has been laid to develop techniques to determine how the tissue in the lung moves. We intend to quantify the extent to which lung tissue moves similarly to the surrounding anatomy, and the implications this has on fiducial/target proximity.

II. METHODS AND MATERIALS

II.A Dataset and techniques

Ten randomly chosen primary lung cancer patients underwent IRB approved 4DCT scans in the supine position. The scans were performed using a Philips Brilliance 16 slice CT scanner (Philips Medical Systems) that was operated in ciné mode with a stationary couch during the scan. Ciné as opposed to helical acquisition was selected in order to perform amplitude-based reconstruction. The axial slice thickness was set at 1.5 mm, which yielded a total thickness of 24 mm for each couch position (16 slices × 1.5 mm/slice). For each axial slice, 25 images were acquired over the course of two to three breathing cycles. Respiration was monitored using spirometry and a pneumatic bellows pressure sensor attached to the patient's abdomen.[14] A spirometer gives accurate calibrated tidal volume information, however, without the use of a simultaneous bellows signal the spirometer is subject to drift. Each acquired image was synchronized with a corresponding tidal volume as measured by respiratory monitoring devices. The 4DCT scans were reconstructed at maximum inspiration and maximum expiration using amplitude-based reconstruction techniques described previously.[15] The decision to use only maximum inspiration and maximum expiration was based on the fact that previously published results have shown that hysteresis is typically less of a factor than tidal volume related motion.[16] Additionally, applying our model to a higher number of 4DCT phases proved computationally infeasible.

Each 4DCT dataset was imported into clinical treatment planning software (PINNACLE v. 8.0u, Philips Medical). The tumor and four main lobes of the lung (right/left upper/lower) were contoured at exhalation. The right middle lobe was not contoured due to its lack of size. Both inhalation and exhalation scans, along with the contours, were exported and loaded into custom software developed in MATLAB (2007, The MathWorks) in order to perform deformable registration.[17]

Deformable registration was performed using the Horn-Schunck optical flow algorithm[18] in order to obtain motion vectors between exhalation and inhalation for each voxel within the thoracic cavity. After the vectors were obtained for each patient, they were manually inspected to ensure the vector magnitude increased near the diaphragm and the motion vectors matched with the motion of internal high contrast landmarks, such as bronchial branch points. Each scan was reviewed in detail by one of the authors (RS). Errors from deformable registration were found to be comparable to previously published work (~1 mm).[19]

Once the vectors were manually verified, two studies were performed. In the first study, a series of regularly spaced seed points (every 4th voxel. 4 mm spacing lateral and anterior/posterior with 6 mm spacing superior inferior) throughout each lobe were selected to determine the degree of correlation with surrounding tissue motion. In the second study, "tumor-centric" analysis was performed to evaluate the effects of increased rigidity associated with cancerous tissue on motion vector correlation in areas surrounding a tumor.

II.B Methods: Correlation radius

A region growing algorithm was employed to determine the maximum radius at which the magnitude of the vector motion of 95% of the voxels surrounding a seed point correlated to within 3 mm of the motion of the seed voxel (Fig. 1). The technique for the correlation radius analysis is outlined in Fig. 1. A seed point array with 4 mm spacing in the lateral and anterior/posterior directions and 6 mm spacing in the superior/inferior directions was analyzed. For each seed point, the region growing algorithm expanded radially with an increment (Δr) of 1 mm. After each iteration, the exhalation to inhalation motion vectors within the spherical region surrounding the seed point were compared to the motion of the seed voxel. If the motion vector for a given voxel correlated to within the spatial threshold (3 mm) when compared with the motion of the seed voxel, the voxel was considered accepted via our criteria. The spherical region expanded to the maximum radius value at which 95% of the voxels within the region correlated to within 3 mm. Voxels not within the same lung lobe as the seed voxel were disregarded.

II.C Methods: Tumor correlation

In order to quantitatively analyze whether the increased rigidity associated with cancerous tissue affects the surrounding

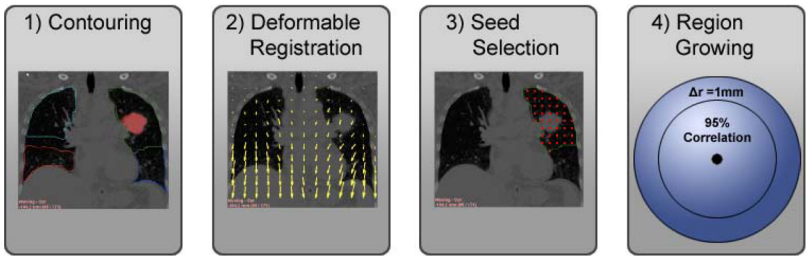

FIG. 1. Model Flowchart. After 4DCT acquisition is performed, lung lobes and the tumor are contoured (1). Deformable registration is performed to generate motion vectors between inhalation and exhalation for each voxel within the thoracic cavity (2). Seeds are selected at regularly spaced intervals within each lung (3). A region growing algorithm determines the maximum radius in which 95% of the voxels correlate to within 3 mm (4).

TABLE I. Correlation radii values to represent 3 mm motion. Means and standard deviations are reported for each lobe. Tumor correlation radii were significantly higher ($p = 0.008$) than the healthy lung tissue radii values.

	Mean	Standard deviation
Left lower	1.7 (cm)	1.1 (cm)
Right lower	1.6	1.1
Left upper	2.1	1.0
Right upper	2.9	1.8
Tumor	3.1	1.8

tissue correlation, the volumetric centroid of the tumor was selected as the representative tumor motion vector. This vector represents the offset of the tumor between maximum exhalation and maximum inhalation. The motion vector from the tumor centroid was compared with the motion vectors of all surrounding tissue within the lungs. If it is assumed that a given voxel moves in a rigid manner with respect to the tumor centroid, this difference effectively represents the intrafraction motion error if a fiducial was placed at that voxel. Differences in the tumor motion vector and the surrounding tissue were plotted using color overlays indicating the motion correlation of surrounding tissue motion with that of the tumor.

III. RESULTS

III.A Results: Correlation radius

Correlation radius values were obtained for each patient. In one patient (35), the motion within the upper right lobe was minimal and hence the vectors correlated to within 3 mm regardless of seed point position. The radius values for this patient were set at the maximum radius value (7 cm). The mean correlation radii for each lobe are shown in the Table I. Additionally, histograms of the radii values for each lobe can be found in Fig. 2. Tumor correlation radii values were found to be higher than those of healthy lung tissue ($p = 0.008$) indicating that the increased rigidity associated with cancerous tissue makes surrounding lung tissue motion highly correlated. Additionally, the upper lobes were found to have radii values significantly higher than the lower lobes ($p < 0.05$); due to the lower overall motion of the upper lobes.

Correlation maps were made for each patient (Fig. 3). The maps show a coronal view taken at the carina. For each map, the interpolated correlation radii for each voxel are overlaid. The correlation with surrounding tissue varies substantially with position and, qualitatively, is inversely related to the divergence of the motion vector field.

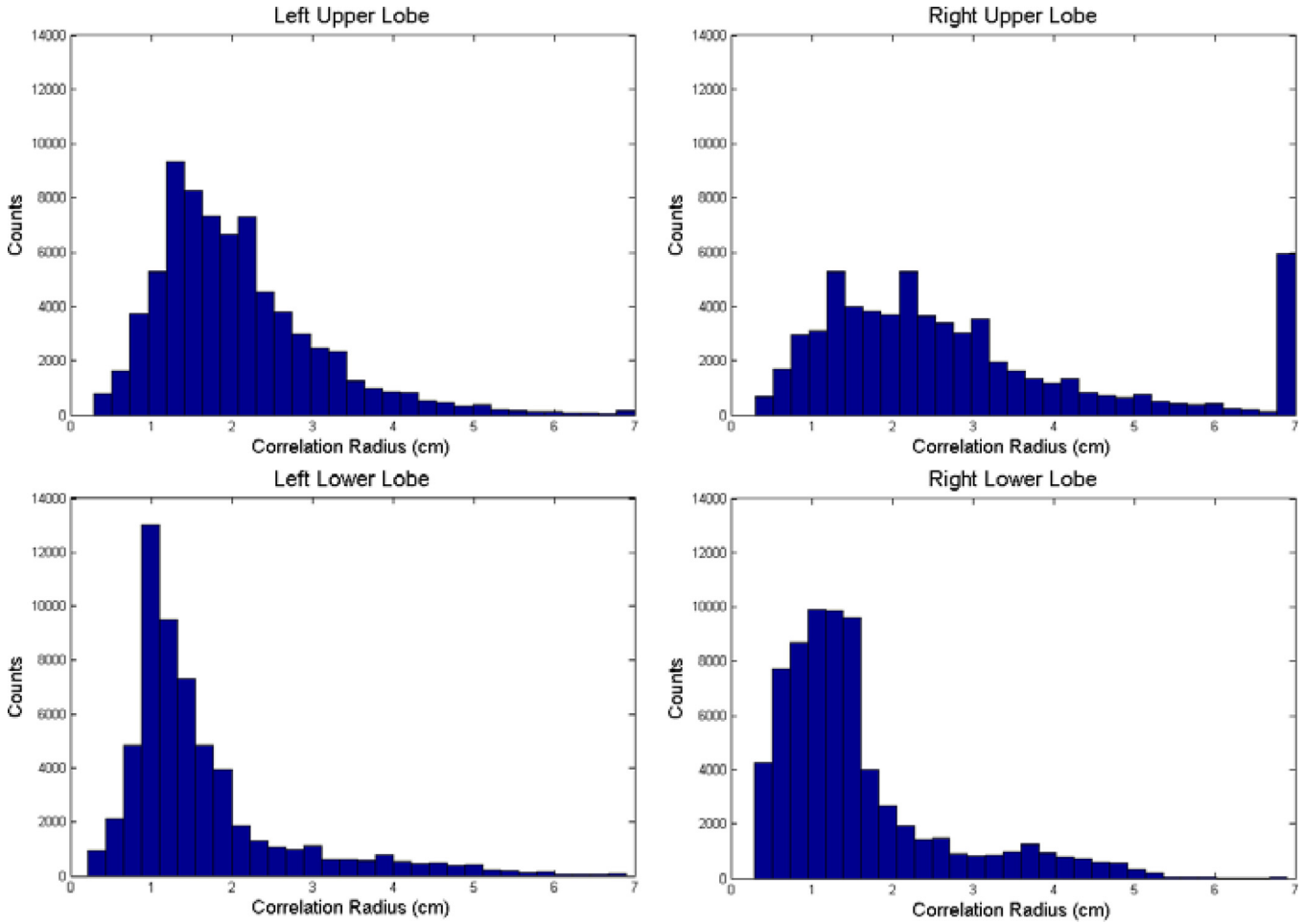

FIG. 2. Histograms of radii values for each lobe. Notice increased correlation radii values for the upper lobes when compared to the lower lobes. Correlation radii values were capped at 7 cm, which resulted in the 7 cm peak in the low motion Right upper lobe.

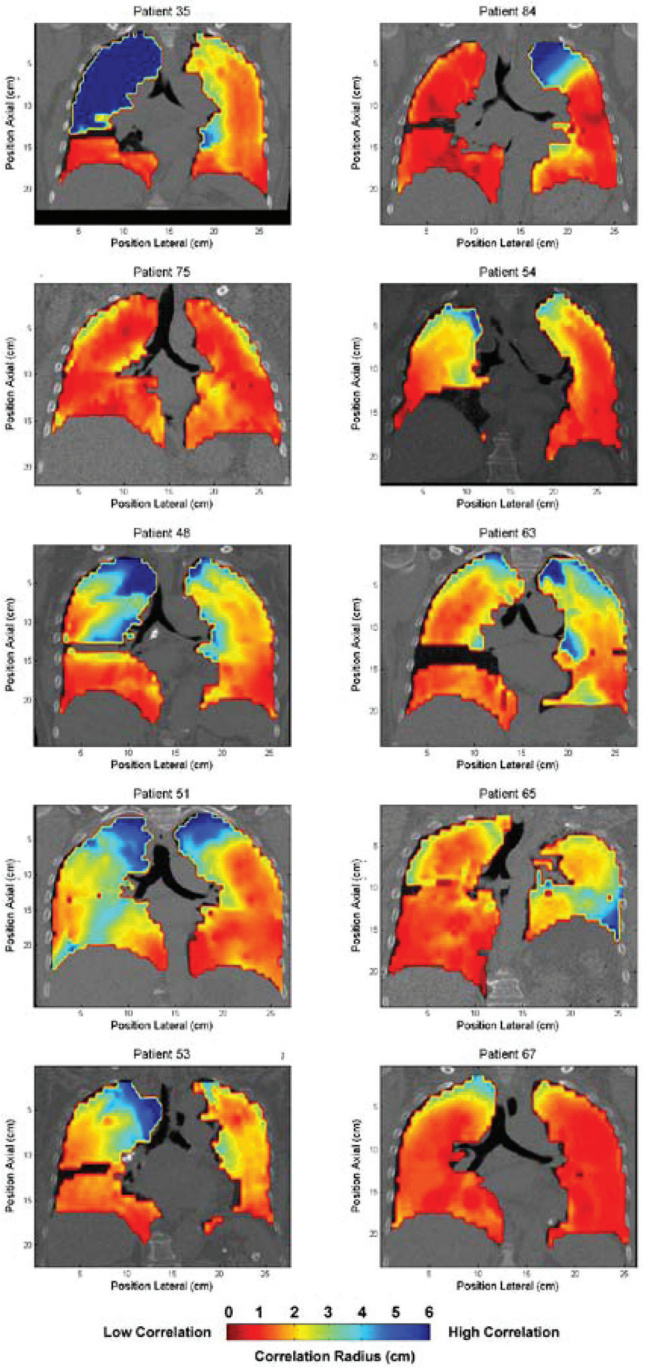

FIG. 3. Correlation radii maps. Regularly spaced voxel within the lung were analyzed using the process described in Fig. 1. Correlation maps were produced to display how well the anatomy correlates with adjacent anatomy within the thoracic cavity. Red indicates low correlation with surrounding anatomy motion, blue indicates high correlation.

As expected, both lower lobes exhibit smaller correlation radii than the upper lobes. This is due to an increase in both the magnitude of the motion near the diaphragm and the divergence of the motion. A higher divergence will decrease the correlation with surrounding anatomy for a given point in the lung, necessitating closer implantation of a fiducial to the target tumor.

III.B Results: Tumor correlation

Correlation values between the volumetric centroid of the tumor and the surrounding tissue are plotted in Fig. 4. Spatial variations in tumor motion correlation with surrounding tissue are evident due to local variations in the divergence of the motion vector field.

Additionally, the correlation error with respect to offset from the tumor centroid is plotted (Fig. 5). The errors were obtained by comparing the motion of the tumor centroid with that of the surrounding anatomy. As expected, correlation deteriorates as one moves further away from the tumor. The tumors ranged in size from radii values of 8 to 32 mm with an average radius of 17 mm.

IV. DISCUSSION

A general rule was not established for where to implant fiducials with respect to the tumor, however, some general guidelines were observed. First, higher correlation radii existed between voxels in the upper lobes as compared with the lower lobes ($p < 0.05$). Second, the correlation radii are higher with respect to the tumor as opposed to randomly selected voxels in the lung ($p < 0.05$). Though this paper only shows the results on ten tumors, this may be due to the increased rigidity of the tumor in the lung parenchyma.

Results show that correlation typically deteriorates when moving in the superior/inferior direction. This is the largest component vector of respiratory motion and generally the largest component of the divergence. A lateral spatial offset from the tumor often provided regions with correlated motion (Fig. 4, Patients 53 and 35); however, some patients showed increased correlation in the superior/inferior direction (Fig. 4, Patients 51 and 84). Internal motion correlation is highly patient specific as well as specific to the lobe and location within the lung.

It is evident that the extent at which surrounding tissue motion correlates with an internal point within the lung is highly variable, both from patient to patient as well as from point to point within a single patient. Though this study confirms that the closer the fiducial is implanted, the better it represents tumor motion, it also shows that in many patient situations a fiducial that is within 3 cm of the tumor would represent tumor motion within 3 mm. Virtually all (95%) of the surrounding voxels move the same as the seed point. It is important to remember that the study was limited to the exhale and inhale voxels only; and there could possibly be points during the motion trajectory where the fiducial did not represent the tumor motion within 3 mm.

There are potential concerns with using implanted fiducials in the lung. Foreign objects inside the body produce an immune response, however, prior studies have shown that this response clinically acceptable for most cases.[20–22] Additionally, fiducial migration is a concern. Our group has published work with a modified transponder design which shows a 100% fixation rate within the lung for 54 fiducials.[23] Other groups have published results using gold seeds which show comparable fixation rates (120/123[21], 11/11[24], 10/10[4]). Internal anatomy tends to shrink as a result of radiation

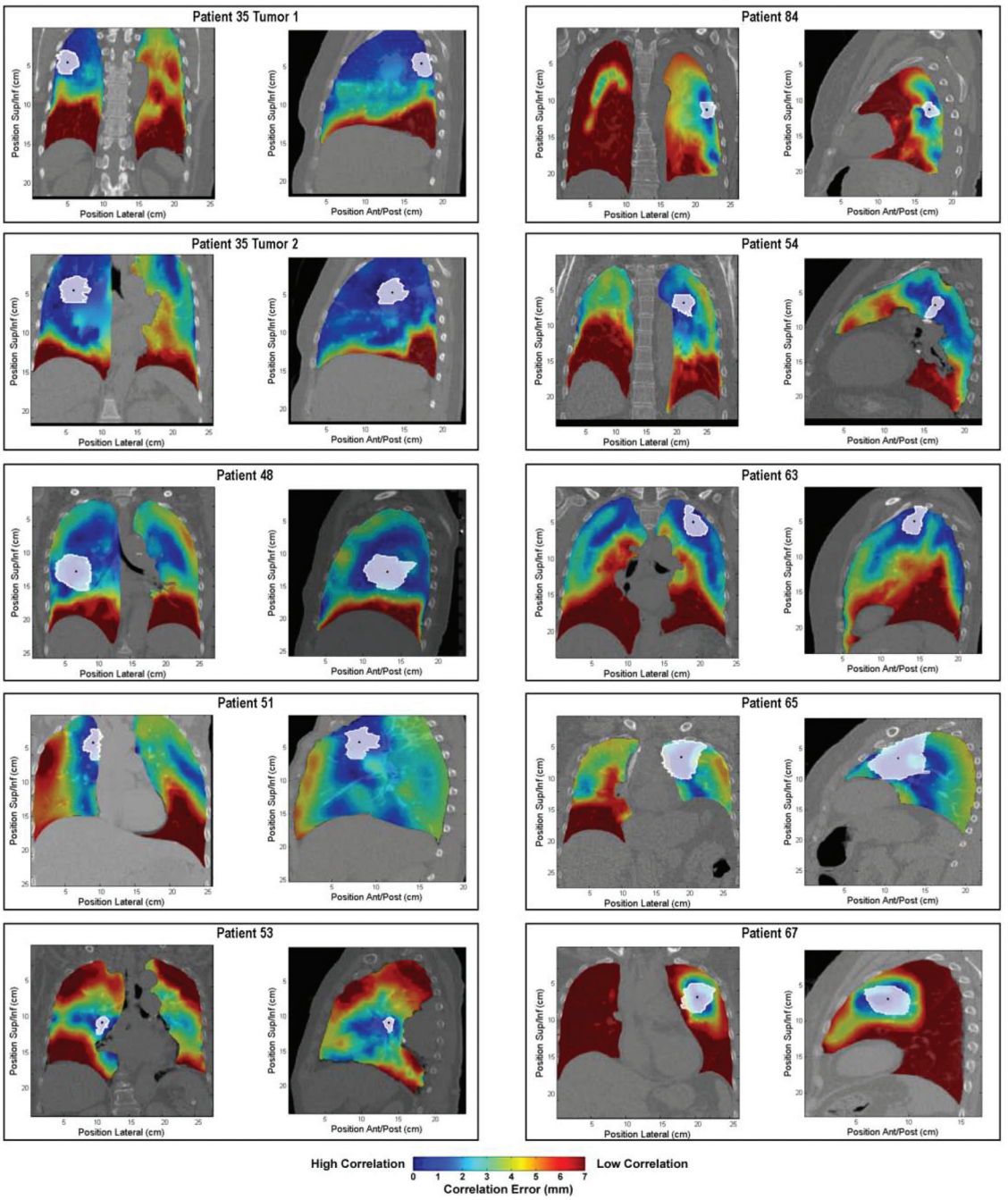

FIG. 4. Tumor correlation maps. Tumor boundaries are outlined in white, with the centroid indicated with a black point. Correlation with surrounding tissue is indicated by color with high correlation as blue and low correlation as red.

therapy, and without adaptive planning this has the potential to lead to differences in tumor/fiducial correlation between initial planning and the completion of treatment. This is a question that is currently being actively researched but remains unanswered.

The benefits of implanted fiducials are substantial. Internal fiducials, as compared with external respiratory surrogates, can assist in decreasing both error associated with patient setup as well as respiratory motion.[5] Additionally, numerous applications aimed at mitigating intrafraction motion within the lung have been published using internal fiducials as a respiratory surrogate.[5,8–10,25] For motion management techniques such as respiratory gating that rely only on tumor/fiducial correlation during a specified phase-amplitude of the breathing cycle, the relative motion between the fiducial and tumor is potentially irrelevant during BEAM-OFF. However, for highly efficient techniques that treat throughout the respiratory cycle, a continuous knowledge of the tumor/fiducial relationship is necessary. Adding increased confidence in localizing a target within the lung can offer a reduction in PTV margins in an effort to spare healthy tissue.[26]

In conclusion, our study shows variable radii around different points in the lung where a fiducial would follow a

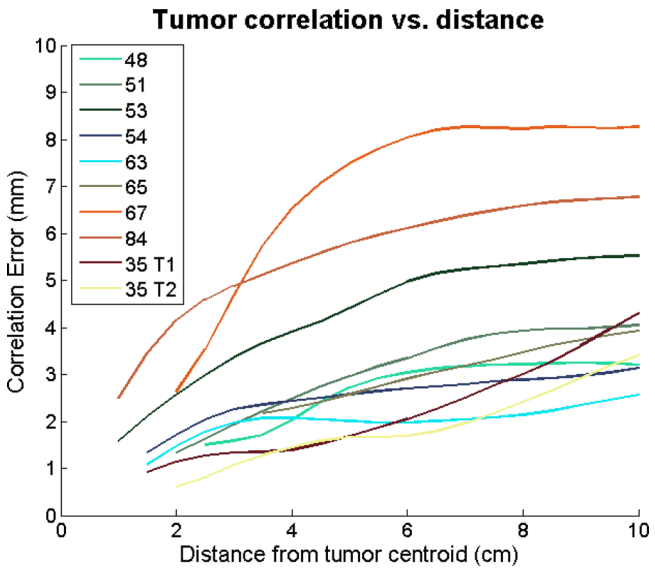

FIG. 5. Tumor correlation vs. offset. Motion correlation errors increase as the distance from the tumor centroid increases. Curves for each patient start at the mean tumor radius.

tumor within 3 mm. The correlation radii are much larger around the tumors as compared with normal lung tissue. Clinical decisions such as reducing PTV margins due to an internal fiducial based motion management solution should account for both the error associated with the internal fiducial tracking system, as well as the error associated with tumor/fiducial correlation as determined by patient specific respiratory correlated imaging after fiducial placement.

Disclosures: Parag Parikh receives research funds from Calypso Medical, Martin Mayse works as a consultant to Calypso Medical. Supported in part by R01CA096679 and R01CA134541.

[a]Author to whom correspondence should be addressed. Electronic mail: pparikh@radonc.wustl.edu

[1]P. M. Chi *et al.*, "Relation of external surface to internal tumor motion studied with cine CT," Med. Phys. **33**, 3116–3123 (2006).
[2]R. I. Berbeco *et al.*, "Residual motion of lung tumours in gated radiotherapy with external respiratory surrogates," Phys. Med. Biol. **50**, 3655–3667 (2005).
[3]D. P. Gierga *et al.*, "The correlation between internal and external markers for abdominal tumors: implications for respiratory gating," Int. J. Radiat. Oncol., Biol., Phys. **61**, 1551–15558(2005).
[4]P. A. Kupelian *et al.*, "Implantation and Stability of Metallic Fiducials Within Pulmonary Lesions," Int. J. Radiat. Oncol., Biol., Phys. **69**, 777–785 (2007).
[5]H. Shirato *et al.*, "Physical aspects of a real-time tumor-tracking system for gated radiotherapy," Int. J. Radiat. Oncol., Biol., Phys. **48**, 1187–1195 (2000).
[6]P. Kupelian *et al.*, "Multi-institutional clinical experience with the Calypso System in localization and continuous, real-time monitoring of the prostate gland during external radiotherapy," Int. J. Radiat. Oncol., Biol., Phys. **67**, 1088–1098 (2007).
[7]T. R. Willoughby *et al.*, "Target localization and real-time tracking using the Calypso 4D localization system in patients with localized prostate cancer," Int. J. Radiat. Oncol., Biol., Phys. **65**, 528–534 (2006).
[8]R. L. Smith *et al.*, "Evaluation of linear accelerator gating with real-time electromagnetic tracking," Int. J. Radiat. Oncol., Biol., Phys. **74**, 920–927 (2009).
[9]R. L. Smith *et al.*, "Integration of real-time internal electromagnetic position monitoring coupled with dynamic multileaf collimator tracking: An intensity-modulated radiation therapy feasibility study," Int. J. Radiat. Oncol., Biol., Phys. **74**, 868–875 (2009).
[10]A. Sawant *et al.*, "Toward submillimeter accuracy in the management of intrafraction motion: The integration of real-time internal position monitoring and multileaf collimator target tracking," Int. J. Radiat. Oncol., Biol., Phys. **74**, 575–582 (2009).
[11]A. Schweikard *et al.*, "Robotic motion compensation for respiratory movement during radiosurgery," Comput. Aided Surg. **5**, 263–277(2000).
[12]M. J. Murphy, "An automatic six-degree-of-freedom image registration algorithm for image-guided frameless stereotaxic radiosurgery," Med. Phys. **24**, 857–866 (1997).
[13]N. Koch *et al.*, "Evaluation of internal lung motion for respiratory-gated radiotherapy using MRI: Part I—Correlating internal lung motion with skin fiducial motion," Int. J. Radiat. Oncol., Biol., Phys. **60**, 1459–1472 (2004).
[14]W. Lu *et al.*, "Quantitation of the reconstruction quality of a four-dimensional computed tomography process for lung cancer patients," Med. Phys. **32**, 890–901 (2005).
[15]D. A. Low *et al.*, "A method for the reconstruction of four-dimensional synchronized CT scans acquired during free breathing," Med. Phys. **30**, 1254–1263 (2003).
[16]D. A. Low *et al.*, "Novel breathing motion model for radiotherapy," Int. J. Radiat. Oncol., Biol., Phys. **63**, 921–929 (2005).
[17]D. Yang *et al.*, "DIRART—A software suite for deformable image registration and adaptive radiotherapy research," *World Congress on Medical Physics and Biomedical Engineering*, September 7–12 (Munich, Germany, 2009), pp. 844–847 (2009) (available at http://dx.doi.org/10.1007/978-3-642-03474-9_236)
[18]B. K. Horn and B. G. Schunck, "Determining optical flow," Artif. Intell. **17**, 185–203 (1981).
[19]T. Zhao *et al.*, "Characterization of free breathing patterns with 5D lung motion model," Med. Phys. **36**, 5183–5189 (2009).
[20]R. I. Whyte *et al.*, "Stereotactic radiosurgery for lung tumors: Preliminary report of a phase I trial," Ann. Thorac. Surg. **75**, 1097–1101 (2003).
[21]H. Shirato *et al.*, "Feasibility of insertion/implantation of 2.0-mm-diameter gold internal fiducial markers for precise setup and real-time tumor tracking in radiotherapy," Int. J. Radiat. Oncol. Biol., Phys. **56**, 240–247 (2003).
[22]M. Imura *et al.*, "Insertion and fixation of fiducial markers for setup and tracking of lung tumors in radiotherapy," Int. J. Radiat. Oncol. Biol. Phys. **63**, 1442–1447 (2005).
[23]M. Mayse *et al.*, "Development of a non-migrating electromagnetic transponder system for lung tumor tracking," Int. J. Radiat. Oncol., Biol., Phys. **72**, S430 (2008).
[24]T. R. Willoughby *et al.*, "Evaluation of an infrared camera and x-ray system using implanted fiducials in patients with lung tumors for gated radiation therapy," Int. J. Radiat. Oncol., Biol., Phys. **66**, 568–575 (2006).
[25]S. Shimizu *et al.*, "Detection of lung tumor movement in real-time tumor-tracking radiotherapy," Int. J. Radiat. Oncol., Biol., Phys. **51**, 304–310 (2001).
[26]J. Mechalakos *et al.*, "Dosimetric effect of respiratory motion in external beam radiotherapy of the lung," Radiother. Oncol. **71**, 191–200 (2004).